AIAA 2004-3675

On the Bidirectional Vortex and Other Similarity Solutions in Spherical Geometry

J. Majdalani and D. Fang
Advanced Theoretical Research Center
University of Tennessee Space Institute
Tullahoma, TN 37388

S. W. Rienstra
Eindhoven University of Technology
NL-5600 MB Eindhoven, Netherlands

40th AIAA/ASME/SAE/ASEE Joint Propulsion Conference and Exhibit
11–14 July 2004
Fort Lauderdale, FL

40th AIAA/ASME/SAE/ASEE Joint Propulsion Conference and Exhibit
11-14 July 2004, Fort Lauderdale, Florida

AIAA 2004-3675

On the Bidirectional Vortex and Other Similarity Solutions in Spherical Geometry

Joseph Majdalani* and Dianqi Fang†
University of Tennessee Space Institute, Tullahoma, TN 37388
and
Sjoerd W. Rienstra‡
Eindhoven University of Technology, NL-5600 MB Eindhoven, Netherlands

The bidirectional vortex refers to the bipolar, coaxial, two-cell swirling motion that can be triggered, for example, in cyclone separators and some liquid rocket engines with tangential aft-end injectors. In this study, we derive an exact solution to describe the corresponding bulk motion in spherical geometry. Our approach invokes the assumptions of steady, incompressible, inviscid, rotational, and axisymmetric flow. Of the three possible types of similarity solutions that are shown to fulfill the momentum equation, only the second leads to a closed-form analytical expression that satisfies the boundary conditions for the bidirectional vortex in a straight cylinder. While the first type is incapable of satisfying the required conditions, its general form may be used to accommodate other physical settings. This case is illustrated in the context of inviscid flow over a sphere. The third type is more general and provides multiple solutions although it precludes a closed-form analytical outcome except for one case. The spherical bidirectional vortex is derived using separation of variables and the method of variation of parameters. The three-pronged analysis presented here increases our repertoire of general mean flow solutions that rarely appear in spherical geometry. It is hoped that these general forms will enable us to extend the current approach to other complex fluid motions that are simpler to capture using spherical coordinates. One such case corresponds to the analytical treatment of cyclonic flow in a conical chamber, a well known problem that remains unresolved.

Nomenclature

a = chamber radius, $R_i \sin\phi_i$
A_i = inlet area of the incoming swirl flow
b = chamber outlet radius, βa
l = chamber aspect ratio, L/a
p = pressure
Q_i = volumetric flow rate, UA_i
r = radial coordinate in cylindrical geometry
R = radial coordinate in spherical geometry
Re = injection Reynolds number, Ua/ν
R_i = inlet radius measured from head end, $a\csc\phi_i$
S = swirl number, $\pi ab/A_i = \pi\beta\sigma$
$\boldsymbol{u}$ = velocity vector (u_R, u_ϕ, u_θ)
U = tangential injection velocity, $u_\theta(R_i,\phi_i,\theta)$
z = axial coordinate
β = normalized outlet radius, b/a
κ = tangential inlet parameter, $(2\pi\sigma l)^{-1}$
ν = kinematic viscosity, μ/ρ
ρ = density
σ = modified swirl number, $a^2/A_i = S/(\pi\beta)$
$\boldsymbol{\omega}$ = mean flow vorticity, $\nabla\times\boldsymbol{u}$
ψ = mean flow stream function, $\psi(R,\phi)$
ζ = similarity coordinate, $\frac{1}{2}CR^2\sin^2\phi$

Subscripts and Symbols

i = inlet property in the base plane, $z = L$
o = outlet/nozzle property in the base plane, $z = L$
r = radial component in cylindrical geometry
R = radial component in spherical geometry
z = axial component
ϕ = colatitude component
θ = azimuthal component
$\overline{}$ = overbars denote dimensionless quantities

*Jack D. Whitfield Professor of High Speed Flows, Department of Mechanical, Aerospace and Biomedical Engineering. Member AIAA.

†Graduate Research Associate, Marquette University, Department of Mechanical and Industrial Engineering. Member AIAA.

‡Associate Professor, Department of Mathematics and Computing Science. Member AIAA.

I. Introduction

In the last five decades, considerable attention has been given to naturally occurring swirl patterns in thermal and physical transport applications.[1-25] In that vein, different methods have been employed to simulate and trigger swirl in cylindrical or conical chambers using, for example, tangential fluid injection, inlet swirl vanes, aerodynamically-shaped swirl blades, propellers, vortex trippers, twisted tape inserts, coiled wires, vortex generators, and other swirl-prop devices.

Recently, an efficient cooling method has been proposed by Chiaverini and co-workers[26-28] who have managed to reproduce cyclonic motion inside a laboratory-scale liquid rocket engine (see Fig. 1). Their technique is based on inducing a coaxial, co-spinning, bidirectional flow comprising two distinct concentric fields: an outer annular vortex and an inner, tubular vortex. The flow configuration in this chamber is unique in that the oxidizer is injected tangentially into the combustion chamber and just upstream of the nozzle; the process results in a swirling combustion field that exhibits an outer, virtually nonreactive, flow region. This so-called outer vortex fills the annular region separating the combustion core from the chamber walls. The combustion core is formed from the oxidizer mixing and reacting with the fuel. The latter is injected radially or axially at the chamber head end. Before reaching the fuel injection faceplate, the outer vortex remains composed of cool oxidizer; its tendency will be to spiral around while climbing up the chamber walls. The attendant thermal blanket-coil protects the chamber walls from fluctuating heating loads. The direct consequence is that of lowering the wall temperatures to the extent that a laboratory test using a fuel-rich Hydrogen-Oxygen combustion could be safely sustained in a Plexiglas model of this engine.[26-28] The thermal protection feature not only reduces cooling requirements but leads to appreciable cost reduction, prolonged life, more flexibility in material selection, and reduced weight. The inner vortex, on the other hand, plays an important role in improving combustion efficiency. The inner swirl increases fuel residence time, mixing, and turbulence, thus improving overall efficiency and ballistic performance. The spinning vortices provide an extended flow path that exceeds the geometric length of the chamber, thus taking full advantage of the chamber's volumetric capacity.

The utilization of bidirectional vortex motion is, in fact, a well established technology that dates back to the 1950s. Earliest experimental investigations may be credited to the work of ter Linden[1] on dust separators and the treatment of hydraulic and gas cyclones by Kelsall[2] and Smith.[3,4] Theoretical analyses have also been carried out by Fontein and Dijksman,[5] Smith,[3,4] and Bloor and Ingham.[6-8] Semi-empirical models are, in turn, available from Reydon and Gauvin,[9] Vatistas, Lin and Kwok,[10,11] Vatistas,[12] and others. In view of progressive advances in computing, numerical simulations have been recently prompted by Hsieh and Rajamani,[13] Hoekstra, Derksen and Van den Akker,[14] Derksen and Van den Akker,[15] and Fang, Majdalani and Chiaverini.[16]

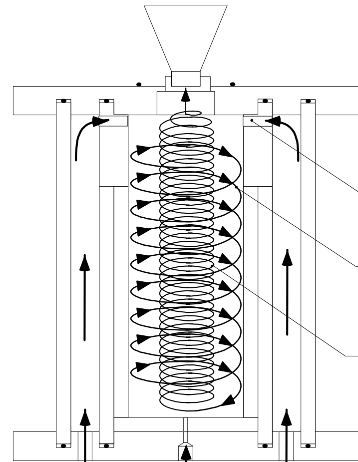

Fig. 1 Schematic of the Cool Wall Bidirectional Vortex Combustion Chamber (CWBVCC) by Chiaverini and co-workers.[26-28]

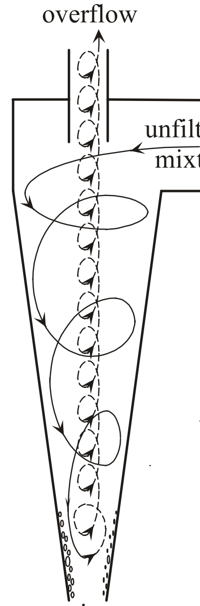

Fig. 2 Schematic of a conical cyclone separator depicting its key components.

Generally, cyclone technology is implemented in coal gas purificators, spray dryers, oil-water separators, gas scrubbers, gas dedustors, hydrocyclones, and magneto-hydrodynamic gas core nuclear rockets. Some are widely used in the petrochemical and powder processing industries where they are employed in catalyst or product recovery, scrubbing, and dedusting. The typical cyclone separator consists of an upper cylindrical can with a central outlet tube and a lower conical section with bottom opening (see Fig. 2). An involute inlet section permits the tangential injection of liquid or gaseous mixtures. The spinning centrifugal motion causes denser and coarser particles to gather along the conical walls. Heavier particles precipitate at the base of the cyclone, the so-called spigot, where the corresponding underflow is withdrawn.

The main difference between a purely cyclonic flow and that reproduced inside the NASA sponsored Cool Wall Bidirectional Vortex Combustion Chamber (CWBVCC) is that the latter exhibits only one outlet section (Fig. 1 versus 2). This difference is minor because the presence of a secondary outlet does not alter the bulk flow motion. The spigot serves as a collection cavity through which heavy particles may be trickled and filtered out of the mixture. The spigot does not affect the main characteristics of the swirling stream inside the cyclone, especially under high speed condition for which friction can be discounted.

The purpose of this study is to explore the general form of the solution for the bidirectional vortex that can be used to describe cyclonic motion in spherical geometry under steady, inviscid, incompressible, rotational, and axisymmetric flow conditions. This investigation will be guided, in part, by the work of Vyas, Majdalani and Chiaverini.[29] In the process, the inviscid momentum equation will be shown to exhibit three possible solutions. These will be considered one-by-one and solved either analytically or numerically.

II. Mathematical Model

In seeking a solution for steady, inviscid, rotational flowfields, it is customary to use the vorticity-stream function approach.[30] Accordingly, one solves

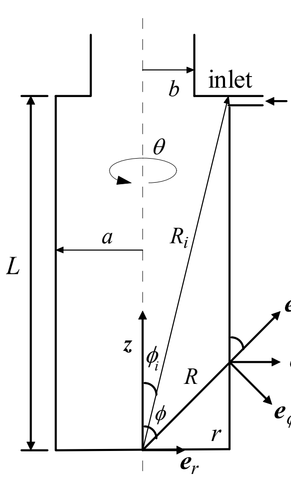

Fig. 3 Spherical coordinate system anchored at the chamber's head end.

$\nabla\times(\boldsymbol{u}\times\boldsymbol{\omega})=0$ and $\boldsymbol{\omega}=\nabla\times\boldsymbol{u}$. While solutions in Cartesian or cylindrical coordinates are quite common, those in spherical geometry remain a rarity. In the present work, the bidirectional vortex will be formulated using the spatial coordinates (R,ϕ,θ) shown in Fig. 3.

A. Governing Equations

In an axisymmetric field in which changes in the $\theta-$directions are small, the equation for continuity reduces to

$$\nabla\cdot\boldsymbol{u}=0 \text{ or } \frac{\partial}{\partial R}\left(R^2\sin\phi u_R\right)+\frac{\partial}{\partial\phi}\left(R\sin\phi u_\phi\right)=0 \quad (1)$$

where u_R and u_ϕ are the two components of the velocity vector $\boldsymbol{u}$. A stream function $\psi(R,\phi)$ that satisfies Eq. (1) can be defined as

$$\frac{\partial\psi}{\partial\phi}=R^2\sin\phi u_R\,,\quad \frac{\partial\psi}{\partial R}=-R\sin\phi u_\phi \quad (2)$$

Next, Euler's momentum equation can be reduced to the vorticity transport equation following the usual steps. Starting with

$$(\boldsymbol{u}\cdot\nabla)\boldsymbol{u}=-\nabla p/\rho \quad (3)$$

one may use the vector identity for the convective term by putting

$$\nabla(\tfrac{1}{2}\boldsymbol{u}^2)-\boldsymbol{u}\times(\nabla\times\boldsymbol{u})=-\nabla p/\rho$$

or

$$\nabla(\tfrac{1}{2}\boldsymbol{u}^2+p/\rho)-\boldsymbol{u}\times(\nabla\times\boldsymbol{u})=0 \quad (4)$$

The curl of the above yields

$$\nabla\times[\boldsymbol{u}\times(\nabla\times\boldsymbol{u})]=0 \text{ or } \nabla\times(\boldsymbol{u}\times\boldsymbol{\omega})=0 \quad (5)$$

Equation (5) is the steady vorticity transport equation that fulfills the conservation of momentum principle.

B. Boundary Conditions

The boundary conditions for the confined bidirectional vortex are granted by:

(1) Tangential inlet at the wall; namely,

$$Q_i=u_\theta(R_i,\phi_i)A_i=UA_i \quad (6)$$

where

$$\phi_i=\tan^{-1}(a/L)\,;\; R_i=\sqrt{L^2+a^2} \quad (7)$$

(2) No flow penetration at the head end; this condition translates into

$$\phi=\tfrac{1}{2}\pi,\forall R\in\left[0,a\right];\; u_\phi\left(R,\tfrac{1}{2}\pi\right)=0 \quad (8)$$

(3) Axisymmetry; this condition prevents flow crossing of the axis when

$$\phi = 0\,;\; u_\phi\left(R,0\right) = 0 \tag{9}$$

(4) No flow penetration at the sidewall; this requires setting

$$R\sin\phi = a\,;\; u_n = u_R \sin\phi + u_\phi \cos\phi = 0 \tag{10}$$

(5) And, finally, global mass balance; the outflow will match the inflow when

$$Q_o = Q_i = UA_i\,,\; u_z = u_R \cos\phi - u_\phi \sin\phi \tag{11}$$

C. Swirl Component

In order to capture the general behavior of the spin velocity u_θ, it is useful to consider the $\theta-$momentum equation. By virtue of the attendant assumptions, one is left with

$$\left(u_R \frac{\partial}{\partial R} + \frac{u_\phi}{R}\frac{\partial}{\partial \phi}\right)(u_\theta R\sin\phi) = 0 \tag{12}$$

This can be expanded into

$$\frac{1}{R^2 \sin\phi}\left[\frac{\partial\psi}{\partial\phi}\frac{\partial(u_\theta R\sin\phi)}{\partial R} - \frac{\partial\psi}{\partial R}\frac{\partial(u_\theta R\sin\phi)}{\partial\phi}\right] = 0 \tag{13}$$

Then, it can be rearranged such that

$$\frac{\partial\psi}{\partial\phi}\frac{\partial(u_\theta R\sin\phi)}{\partial R} - \frac{\partial\psi}{\partial R}\frac{\partial(u_\theta R\sin\phi)}{\partial\phi} = 0 \tag{14}$$

Equation (14) will hold if

$$u_\theta R\sin\phi = f(\psi) \tag{15}$$

because

$$\frac{\dfrac{\partial(u_\theta R\sin\phi)}{\partial\phi}}{\dfrac{\partial\psi}{\partial\phi}} = \frac{\dfrac{\partial(u_\theta R\sin\phi)}{\partial R}}{\dfrac{\partial\psi}{\partial R}} = f'(\psi) \tag{16}$$

In order to further satisfy Eq. (6), a free vortex form must be exhibited by the swirling velocity. One finds, for constant f

$$u_\theta = U\frac{R_i \sin\phi_i}{R\sin\phi} \tag{17}$$

D. Vorticity-Stream Function Approach

Because u_θ does not appear in the continuity equation, one may invoke the vorticity-stream function approach and replace the remaining components of velocity using

$$u_R = \frac{1}{R^2 \sin\phi}\frac{\partial\psi}{\partial\phi}\,,\;\; u_\phi = -\frac{1}{R\sin\phi}\frac{\partial\psi}{\partial R} \tag{18}$$

The corresponding vorticity becomes

$$\boldsymbol{\omega} = \omega_R \boldsymbol{e}_R + \omega_\phi \boldsymbol{e}_\phi + \omega_\theta \boldsymbol{e}_\theta = \frac{1}{R}\left[\frac{\partial}{\partial R}(Ru_\phi) - \frac{\partial u_R}{\partial\phi}\right]\boldsymbol{e}_\theta \tag{19}$$

Having realized that the inviscid vorticity gives a single component in the swirl direction, $\omega = \omega_\theta$, one may drop the subscript θ and write

$$\omega = \frac{1}{R}\frac{\partial}{\partial R}(Ru_\phi) - \frac{1}{R}\frac{\partial u_R}{\partial\phi} \tag{20}$$

Substitution into the vorticity transport equation requires evaluating

$$\nabla\times(\boldsymbol{u}\times\boldsymbol{\omega}) = -\left[\frac{1}{R}\frac{\partial(R\omega u_R)}{\partial R} + \frac{1}{R}\frac{\partial(\omega u_\phi)}{\partial\phi}\right]\boldsymbol{e}_\theta \tag{21}$$

According to the vorticity transport relation given in Eq. (5), one must put

$$\frac{\partial(R\omega u_R)}{\partial R} + \frac{\partial(\omega u_\phi)}{\partial\phi} = 0 \tag{22}$$

hence

$$\frac{\partial}{\partial R}\left(\frac{\omega}{R\sin\phi}\frac{\partial\psi}{\partial\phi}\right) - \frac{\partial}{\partial\phi}\left(\frac{\omega}{R\sin\phi}\frac{\partial\psi}{\partial R}\right) = 0 \tag{23}$$

This can be expanded as

$$\frac{\partial\left(\dfrac{\omega}{R\sin\phi}\right)}{\partial R}\frac{\partial\psi}{\partial\phi} - \frac{\partial\left(\dfrac{\omega}{R\sin\phi}\right)}{\partial\phi}\frac{\partial\psi}{\partial R} = 0 \tag{24}$$

then rearranged into

$$\frac{\dfrac{\partial\left[\omega/\left(R\sin\phi\right)\right]}{\partial R}}{\dfrac{\partial\left[\omega/\left(R\sin\phi\right)\right]}{\partial\phi}} = \frac{\dfrac{\partial\psi}{\partial R}}{\dfrac{\partial\psi}{\partial\phi}} \tag{25}$$

As usual, the vorticity transport equation will be true if

$$\frac{\omega}{R\sin\phi} = f(\psi) \tag{26}$$

In general, a solution of the form $f(\psi) = C\psi^\lambda$ may be sought. Three cases are readily distinguished depending on the exponent λ. Specifically, three different types of solutions may be defined viz.

$$\lambda = \begin{cases} 0; & \text{type I} \\ 1; & \text{type II} \\ \text{other}; & \text{type III} \end{cases} \tag{27}$$

III. Possible Solutions

The suitability of Eq. (27) to describe the bidirectional vortex motion must, of course, be tested. We begin by considering the simplest form attempted by researchers, namely, the $\lambda = 0$ case.

A. Type I Solution: Potential Flow Past a Sphere

For $\lambda = 0$, one obtains $f(\psi) = C$; the vorticity becomes independent of the stream function. Equation (26) yields $\omega = CR\sin\phi$, which can be readily substituted into Eq. (20). The result can be simplified using Eq. (2) and put in the form

$$\frac{\partial^2\psi}{\partial R^2} + \frac{\sin\phi}{R^2}\frac{\partial}{\partial\phi}\left(\frac{1}{\sin\phi}\frac{\partial\psi}{\partial\phi}\right) + CR^2\sin^2\phi = 0 \quad (28)$$

Assuming a separable solution of the form $\psi = F(R)\sin^2\phi$, it can be shown that

$$R^2F''(R) - 2F(R) = -CR^4 \quad (29)$$

and so

$$F(R) = C_1R^2 + \frac{C_2}{R} - \frac{C}{10}R^4 \quad (30)$$

A generalized type I stream function corresponding to this case is hence unraveled, specifically,

$$\psi = \left(C_1R^2 + \frac{C_2}{R} - \frac{C}{10}R^4\right)\sin^2\phi \quad (31)$$

Unfortunately, this form cannot accommodate the boundary conditions attributed to the bidirectional vortex, given by Eqs. (8)–(11). Instead, Eq. (31) can be readily adapted to describe the flow conditions associated with a uniform flow past a sphere. As illustrated in Fig. 4, this classic problem exhibits rather simple boundary conditions. In the far field, one has

$$R \to \infty\,,\ \psi \to \tfrac{1}{2}UR^2\sin^2\phi + \text{const} \quad (32)$$

so that

$$C = 0 \ \text{ and } \ C_1 = \tfrac{1}{2}U \quad (33)$$

The immediate implication here is that of an irrotational flow since $\omega = CR\sin\phi = 0$. The corresponding stream function reduces to

$$\psi = \left(\tfrac{1}{2}UR^2 + \frac{C_2}{R}\right)\sin^2\phi \quad (34)$$

The remaining constant can be obtained from the hard wall boundary condition along the sphere's radius.

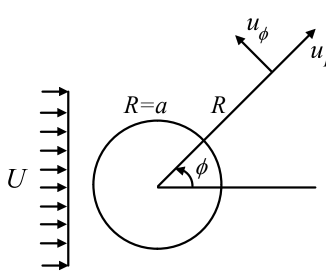

Fig. 4 The case of uniform flow past a sphere leading to an inviscid, irrotational solution.

Given that $\psi(a,\phi) = 0$, one must have

$$C_2 = -\tfrac{1}{2}Ua^3 \quad (35)$$

This leaves us with the familiar solution

$$\psi = \tfrac{1}{2}UR^2\sin^2\phi\left(1 - \frac{a^3}{R^3}\right) \quad (36)$$

and

$$\begin{cases} u_R = 2U\cos\phi\left(1 - a^3R^{-3}\right) \\ u_\phi = -\tfrac{1}{2}U\sin\phi\left(2 + a^3R^{-3}\right) \end{cases} \quad (37)$$

Equation (37) replicates the potential flow profile past a sphere; it is unsuitable for representing the bidirectional vortex.

B. Type II Solution: Bidirectional Vortex

For $\lambda = 1$, one recovers the classic linear form, $f(\psi) = C^2\psi$. The corresponding vorticity-stream function relation becomes $\omega = C^2\psi R\sin\phi$. Rearward substitution into Eq. (20) gives

$$C^2\psi R\sin\phi = \frac{1}{R}\frac{\partial}{\partial R}\left(Ru_\phi\right) - \frac{1}{R}\frac{\partial u_R}{\partial\phi} \quad (38)$$

This PDE can be fully expressed in terms of the stream function

$$C^2\psi R\sin\phi = \frac{1}{R}\frac{\partial}{\partial R}\left(-\frac{1}{\sin\phi}\frac{\partial\psi}{\partial R}\right) - \frac{1}{R}\frac{\partial}{\partial\phi}\left(\frac{1}{R^2\sin\phi}\frac{\partial\psi}{\partial\phi}\right) \quad (39)$$

and so

$$\frac{\partial^2\psi}{\partial R^2} + \frac{\sin\phi}{R^2}\frac{\partial}{\partial\phi}\left(\frac{1}{\sin\phi}\frac{\partial\psi}{\partial\phi}\right) + C^2\psi R^2\sin^2\phi = 0 \quad (40)$$

Using the product rule, the middle term can be expanded and simplified:

$$\frac{\sin\phi}{R^2}\frac{\partial}{\partial\phi}\left(\frac{1}{\sin\phi}\frac{\partial\psi}{\partial\phi}\right) = \frac{1}{R^2}\left[\frac{\partial^2\psi}{\partial\phi^2} - \frac{\cos\phi}{\sin\phi}\frac{\partial\psi}{\partial\phi}\right] \quad (41)$$

Equation (40) becomes, at length,

$$\frac{\partial^2\psi}{\partial R^2} + \frac{1}{R^2}\frac{\partial^2\psi}{\partial\phi^2} - \frac{1}{R^2}\frac{\cos\phi}{\sin\phi}\frac{\partial\psi}{\partial\phi} + C^2\psi R^2\sin^2\phi = 0 \quad (42)$$

This is the key equation that needs to be solved for type II behavior. Its linearity suggests the possibility of a closed-form solution.

1. Separating the Vorticity Equation

At this stage, it is useful to attempt a similarity solution of the form $\psi(R,\phi) = \psi(\zeta)$ with the similarity variable $\zeta = \tfrac{1}{2}CR^2\sin^2\phi$; this requires evaluating

$$\frac{\partial \zeta}{\partial R} = CR\sin^2\phi; \quad \frac{\partial \zeta}{\partial \phi} = CR^2 \sin\phi\cos\phi \tag{43}$$

Inserting into Eq. (42) yields

$$C\sin^2\phi\psi' + 2C\zeta\sin^2\phi\psi'' - C\sin^2\phi\psi' + 2C\zeta\cos^2\phi\psi'' + 2C\zeta\psi = 0 \tag{44}$$

and so

$$2C\zeta(\sin^2\phi + \cos^2\phi)\psi'' + 2\zeta C\psi = 0 \tag{45}$$

leading to

$$\psi'' + \psi = 0 \tag{46}$$

The standard solution is, of course,

$$\psi = C_1\sin\zeta + C_2\cos\zeta \tag{47}$$

or

$$\psi = C_1\sin(\tfrac{1}{2}CR^2\sin^2\phi) + C_2\cos(\tfrac{1}{2}CR^2\sin^2\phi) \tag{48}$$

Equation (42) is deceptively simple and can be shown to be unsuitable for the bidirectional vortex. The constants of integration must be permitted to vary in order to capture more complex features of the flow. This will be carried out next.

2. *General Behavior of the Type II Solution*

A more general solution for Eq. (42) can be pursued in the spirit of Eq. (48); to that end, one can let

$$\psi = C_1(R,\phi)\sin(\tfrac{1}{2}CR^2\sin^2\phi) + C_2(R,\phi)\cos(\tfrac{1}{2}CR^2\sin^2\phi) \tag{49}$$

This ansatz may be substituted back into Eq. (42); after some algebra, one segregates

$$\left[C\cos\zeta\sin(2\phi)\frac{\partial C_1}{\partial\phi} - \frac{\cot\phi}{R^2}\sin\zeta\frac{\partial C_1}{\partial\phi} + \frac{\sin\zeta}{R^2}\frac{\partial^2 C_1}{\partial\phi^2} + 2CR\cos\zeta\sin^2\phi\frac{\partial C_1}{\partial R} + \sin\zeta\frac{\partial^2 C_1}{\partial R^2}\right]$$
$$-\left[C\sin\zeta\sin(2\phi)\frac{\partial C_2}{\partial\phi} + \frac{\cot\phi}{R^2}\cos\zeta\frac{\partial C_2}{\partial\phi} - \frac{\cos\zeta}{R^2}\frac{\partial^2 C_2}{\partial\phi^2} + 2CR\sin\zeta\sin^2\phi\frac{\partial C_2}{\partial R} - \cos\zeta\frac{\partial^2 C_2}{\partial R^2}\right] = 0 \tag{50}$$

It is interesting to note the striking similarity between bracketed terms in Eq. (50). One is thus able to disentangle particular solutions by first collecting the $\cos\zeta -$ and $\sin\zeta -$ terms, and then causing them to vanish simultaneously. One gathers

$$\cos\phi\sin\phi\frac{\partial C_1}{\partial\phi} + R\sin^2\phi\frac{\partial C_1}{\partial R} = 0 \tag{51}$$

with

$$\frac{\partial^2 C_1}{\partial R^2} + \frac{1}{R^2}\frac{\partial^2 C_1}{\partial\phi^2} - \frac{\cot\phi}{R^2}\frac{\partial C_1}{\partial\phi} = 0 \tag{52}$$

and, in like manner,

$$\cos\phi\sin\phi\frac{\partial C_2}{\partial\phi} + R\sin^2\phi\frac{\partial C_2}{\partial R} = 0 \tag{53}$$

with

$$\frac{\partial^2 C_2}{\partial R^2} + \frac{1}{R^2}\frac{\partial^2 C_2}{\partial\phi^2} - \frac{\cot\phi}{R^2}\frac{\partial C_2}{\partial\phi} = 0 \tag{54}$$

Equation (52) is linear and can be solved using the method of characteristics. One finds that $C_1 = f(R\cos\phi)$. To determine f, one substitutes the relation $C_1 = f(R\cos\phi)$ back into Eq. (52); this operation yields $f''(R\cos\phi) = 0$ or

$$C_1 = f(R\cos\phi) = K_1R\cos\phi + K_2 \tag{55}$$

Using similar arguments and Eqs. (53)–(54), one finds

$$C_2 = K_3R\cos\phi + K_4 \tag{56}$$

One form of the type II stream function satisfying Eq. (42) becomes

$$\psi = (K_1R\cos\phi + K_2)\sin\zeta + (K_3R\cos\phi + K_4)\cos\zeta \tag{57}$$

3. *General Axisymmetric Behavior*

Based on Eqs. (18) and (57), one can re-evaluate the velocity components

$$u_R = \frac{1}{R}\Big\{\big[-K_3 + CK_2R\cos\phi + CK_1R^2\cos^2\phi\big]\times\cos\zeta - \big[K_1 + CK_4R\cos\phi + CK_3R^2\cos^2\phi\big]\sin\zeta\Big\} \tag{58}$$

and

$$u_\phi = -\frac{1}{R}\Big\{\big[K_3\cot\phi + CR\big(K_2 + K_1R\cos\phi\big)\times\sin\phi\big]\cos\zeta + \big[-K_1\cot\phi + C\big(K_4 + K_3R\cos\phi\big)\sin\phi\big]\sin\zeta\Big\} \tag{59}$$

Axisymmetry demands that K_3 and K_4 be zero lest the component of the velocity be unbounded along the axis. At the outset, the general solution appropriate of axisymmetric flows reduces to

$$\psi = \big(K_1R\cos\phi + K_2\big)\sin\zeta \tag{60}$$

with the companion velocities

$$u_R = \frac{1}{R}\left[CR\cos\phi\left(K_1 R\cos\phi + K_2\right)\cos\zeta - K_1\sin\zeta\right] \quad (61)$$

and

$$u_\phi = -\frac{1}{R}\left[CR\sin\phi\left(K_1 R\cos\phi + K_2\right)\cos\zeta + K_1\cot\phi\sin\zeta\right] \quad (62)$$

Equations (61)–(62) represent the type II class of solutions for an axisymmetric flowfield.

4. *Specific Case: Cylindrical Bidirectional Vortex*

A cylindrical cyclone or a CWBVCC chamber may be modeled as a cylindrical tube of length L and radius a; the head end may be considered impermeable (due to the corresponding small volumetric flux associated with the underflow in a cyclone or the fuel injected in the CWBVCC); the aft end may be assumed to be partially open to a straight nozzle of radius b. A sketch of the chamber is given in Fig. 3 where R, ϕ and θ are used to guide spherical variations. Note that the origin of the spherical coordinate system is placed at the center of the chamber head end; alternatively, r and z are used to represent the cylindrical radial and axial coordinates in a coincident reference frame. The fraction of the radius that is open to flow may be defined by $\beta = b/a$ and the chamber's aspect ratio by $l = L/a$.

Excluding axisymmetry (which is already satisfied) the remaining physical conditions described in Eqs. (8)–(11) may now be applied to Eqs. (61)–(62). Firstly, the state of no flow across the head end requires that $u_\phi\left(R, \tfrac{1}{2}\pi\right) = 0$; hence

$$u_\phi = -CC_1 K_2\cos\left(\tfrac{1}{2}CR^2\right) = 0 \quad (63)$$

This is true when $K_2 = 0$ or

$$\psi = K_1 R\cos\phi\sin\zeta \quad (64)$$

One is left with

$$u_R = K_1\left(CR^2\cos^2\phi\cos\zeta - \sin\zeta\right)/R \quad (65)$$

$$u_\phi = -K_1\left(CR^2\cos\phi\sin\phi\cos\zeta + \cot\phi\sin\zeta\right)/R \quad (66)$$

Secondly, one can enforce the no flow across the sidewall where the radius a remains invariant. Accordingly, the component of the velocity normal to the surface must vanish along $R\sin\phi = a$. Based on geometric considerations, the component of velocity u_n normal to the sidewall may be evaluated from

$$u_n = u_R\sin\phi + u_\phi\cos\phi, \quad R = a\csc\phi \quad (67)$$

where

$$u_R = K_1\sin\phi\left[Ca\cot^2\phi\cos(\tfrac{1}{2}Ca^2) - \sin(\tfrac{1}{2}Ca^2)/a\right] \quad (68)$$

and

$$u_\phi = -K_1\sin\phi\left[Ca\cot\phi\cos(\tfrac{1}{2}Ca^2) + \cot\phi\sin(\tfrac{1}{2}Ca^2)/a\right] \quad (69)$$

Equation (67) becomes

$$u_n = -(K_1/a)\sin(\tfrac{1}{2}Ca^2) \quad (70)$$

The no flow across the sidewall requires that $u_n = 0$ or $\sin\left(\tfrac{1}{2}Ca^2\right) = 0$. This condition precipitates

$$C = 2n\pi/a^2, \quad n = 1, 2... \quad (71)$$

Hence, $\psi = K_1 R\cos\phi\sin\left(n\pi a^{-2}R^2\sin^2\phi\right)$. For a single pass bidirectional motion, one must set $n = 1$ such that

$$\psi = K_1 R\cos\phi\sin\left(\pi a^{-2}R^2\sin^2\phi\right) \quad (72)$$

$$\begin{cases} u_R = \dfrac{K_1}{R}\left[2\pi a^{-2}R^2\cos^2\phi\cos\left(\pi a^{-2}R^2 \sin^2\phi\right) - \sin\left(\pi a^{-2}R^2\sin^2\phi\right)\right] \\ u_\phi = \dfrac{-K_1}{R}\left[2\pi a^{-2}R^2\cos\phi\sin\phi\cos\left(\pi a^{-2}R^2 \sin^2\phi\right) + \cot\phi\sin\left(\pi a^{-2}R^2\sin^2\phi\right)\right] \end{cases} \quad (73)$$

The last constant K_1 may be deduced from global mass balance. In Fig. 3, it can be seen that, for flow across a cylindrical face, the axial velocity consists of the combination

$$u_z = u_R\cos\phi - u_\phi\sin\phi \quad (74)$$

such that

$$u_z = \frac{K_1}{R}\left[2\pi a^{-2}R^2\cos^2\phi\cos\left(\pi a^{-2}R^2 \sin^2\phi\right) - \sin\left(\pi a^{-2}R^2\sin^2\phi\right)\right]\cos\phi + \frac{K_1}{R}\left[2\pi a^{-2}R^2\cos\phi\sin\phi\cos\left(\pi a^{-2}R^2 \sin^2\phi\right) + \cot\phi\sin\left(\pi a^{-2}R^2\sin^2\phi\right)\right]\sin\phi \quad (75)$$

This, in turn, simplifies into

$$u_z = 2\pi a^{-2}K_1 R\cos\phi\cos\left(\pi a^{-2}R^2\sin^2\phi\right) = 2\pi a^{-2}K_1 z\cos\left(\pi a^{-2}r^2\right) \quad (76)$$

The global mass balance across the outlet requires that $Q_o = Q_i = UA_i$; hence

$$Q_o = \int_0^b u_z(r, L)2\pi r\,\mathrm{d}r = \int_0^b 4\pi^2 a^{-2}K_1 L\cos(\pi a^{-2}r^2)r\,\mathrm{d}r = 2\pi K_1 L\sin\left(\pi a^{-2}b^2\right) \quad (77)$$

For this to hold, the last constant must be

$$K_1 = \frac{UA_i}{2\pi L \sin\left(\pi a^{-2} b^2\right)} \tag{78}$$

The bidirectional vortex specific to a cylindrical chamber is now at hand. One has

$$\psi = \frac{UA_i R\cos\phi \sin\left(\pi a^{-2} R^2 \sin^2\phi\right)}{2\pi L \sin\left(\pi a^{-2} b^2\right)} \tag{79}$$

with the spherical components

$$u_R = \frac{UA_i}{2\pi RL \sin\left(\pi a^{-2} b^2\right)}\Big[2\pi a^{-2} R^2 \cos^2\phi$$

$$\times\cos\left(\pi a^{-2} R^2 \sin^2\phi\right) - \sin\left(\pi a^{-2} R^2 \sin^2\phi\right)\Big] \tag{80}$$

and

$$u_\phi = \frac{-UA_i}{2\pi RL \sin\left(\pi a^{-2} b^2\right)}\Big[2\pi a^{-2} R^2 \cos\phi \sin\phi$$

$$\times\cos\left(\pi a^{-2} R^2 \sin^2\phi\right) + \cot\phi \sin\left(\pi a^{-2} R^2 \sin^2\phi\right)\Big] \tag{81}$$

This completes the bidirectional vortex representation in spherical geometry. The conical bidirectional vortex is discussed in Appendix A.

C. Type III Solution: Nonlinear Behavior

For $f(\psi) = C^2\psi^\lambda$, $\forall\lambda \neq (0,1)$, a nonlinear relation ensues between the vorticity and stream function. One must reconsider

$$\frac{\partial^2\psi}{\partial R^2} + \frac{\sin\phi}{R^2}\frac{\partial}{\partial\phi}\left(\frac{1}{\sin\phi}\frac{\partial\psi}{\partial\phi}\right)$$

$$+ f(\psi) R^2 \sin^2\phi = 0 \tag{82}$$

with f exhibiting the general form

$$f(\psi) = C\psi^\lambda \tag{83}$$

for some C and λ. If we now assume ψ of the form

$$\psi(R,\phi) = F(R) G(\phi) \tag{84}$$

we get

$$\frac{\mathrm{d}^2 F(R)}{\mathrm{d}R^2} G(\phi) + CF^\lambda(R) G^\lambda(\phi) R^2 \sin\phi$$

$$+ \frac{F(R)\sin\phi}{R^2}\frac{\mathrm{d}}{\mathrm{d}\phi}\left[\frac{1}{\sin\phi}\frac{\mathrm{d}G(\phi)}{\mathrm{d}\phi}\right] = 0 \tag{85}$$

or

$$\frac{R^2}{F(R)}\frac{\mathrm{d}^2 F(R)}{\mathrm{d}R^2} + CF^{\lambda-1} G^{\lambda-1} R^4 \sin^2\phi$$

$$+ \frac{\sin\phi}{G(\phi)}\frac{\mathrm{d}}{\mathrm{d}\phi}\left[\frac{1}{\sin\phi}\frac{\mathrm{d}G(\phi)}{\mathrm{d}\phi}\right] = 0 \tag{86}$$

By applying the transformation $F(R) = H(R)\sqrt{R}$, we are left with

$$\frac{R^2}{F(R)}\frac{\mathrm{d}^2 F(R)}{\mathrm{d}R^2} = -\frac{1}{4} + R\frac{H'}{H} + R^2\frac{H''}{H} \tag{87}$$

In seeking a separable solution, one must equate Eq. (87) to a constant; if this constant is chosen to be $\mu^2 - \frac{1}{4}$, Euler's differential equation is recovered, namely

$$RH' + R^2 H'' = \mu^2 H \tag{88}$$

As usual, the general solution exhibits the form

$$H(R) = AR^\mu + BR^{-\mu} \tag{89}$$

With this information the rest of Eq. (86) becomes independent of R. Instead of using the general solution for H, let us pick

$$H(R) = R^\mu \tag{90}$$

and so

$$\mu^2 - \tfrac{1}{4} + \frac{\sin\phi}{G(\phi)}\frac{\mathrm{d}}{\mathrm{d}\phi}\left[\frac{1}{\sin\phi}\frac{\mathrm{d}G(\phi)}{\mathrm{d}\phi}\right]$$

$$+ CR^{\left(\mu+\frac{1}{2}\right)(\lambda-1)+4} G^{\lambda-1}(\phi)\sin^2\phi = 0 \tag{91}$$

Clearly, Eq. (91) can be made independent of R by choosing

$$\left(\mu + \tfrac{1}{2}\right)(\lambda - 1) + 4 = 0 \tag{92}$$

or

$$\mu = 4/(1-\lambda) - \tfrac{1}{2} \tag{93}$$

This choice turns Eq. (91) into

$$\sin\phi\frac{\mathrm{d}}{\mathrm{d}\phi}\left[\frac{1}{\sin\phi}\frac{\mathrm{d}G(\phi)}{\mathrm{d}\phi}\right] + CG^\lambda(\phi)\sin^2\phi$$

$$+ \left(\mu^2 - \tfrac{1}{4}\right) G(\phi) = 0 \tag{94}$$

The resulting ODE has to be solved subject to the periodicity condition needed for a physically meaningful problem, specifically, $G(0) = G(2\pi)$ and $G'(0) = G'(2\pi)$. This condition places restrictions on the possible choices of C and λ.

Equation (94) is essentially nonlinear because, as it can be seen from Eq. (92), any choice of λ may be possible except for $\lambda = 1$. Using primes to denote differentiation with respect to ϕ, Eq. (94) can be written as

$$G'' - \cot\phi G' + CG^\lambda \sin^2\phi + 4(\lambda+3)(\lambda-1)^{-2} G = 0 \tag{95}$$

Multiple solutions may thus be obtained and those that are meaningful are those that would satisfy the periodicity condition. For example, using $\lambda=-3$, ($\mu=\frac{1}{2}$), and $C=1$, Eq. (95) becomes

$$G''(\phi)-\cot\phi G'(\phi)+G^{-3}(\phi)\sin^2\phi=0 \qquad (96)$$

This can be solved numerically to obtain multiple periodic solutions. The resulting behavior is illustrated in Fig. 5 where it is solved using two sets of initial guesses. These are

$$G_1(\pi/4)=1.558501,\ G_1'(\pi/4)=0.7000145 \qquad (97)$$

and

$$G_2(\pi/4)=4.016863,\ G_2'(\pi/4)=0.05790198 \qquad (98)$$

Note that, for each set, a candidate solution is obtained.

Interestingly, for the special case of $\lambda=-3$, ($\mu=1/2$), an exact solution can be obtained for arbitrary C. This can be seen by reexamining Eq. (94) which now becomes

$$\frac{1}{\sin\phi}\frac{\mathrm{d}}{\mathrm{d}\phi}\left(\frac{1}{\sin\phi}\frac{\mathrm{d}G}{\mathrm{d}\phi}\right)+CG^{-3}(\phi)=0 \qquad (99)$$

By letting $\chi=\cos\phi$ and $G(\phi)=C^{1/4}g(\chi)$, Eq. (99) can be simplified into

$$g''+g^{-3}=0 \qquad (100)$$

where primes are associated with χ. This simple result can be multiplied by g' and integrated to produce

$$\tfrac{1}{2}(g')^2-\tfrac{1}{2}g^{-2}=\text{constant}=\tfrac{1}{2}K_1 \qquad (101)$$

or $g'=\pm\sqrt{K_1+g^{-2}}$. A second integration attempt furnishes

$$\pm\int^g\frac{K_1\xi}{\sqrt{1+K_1\xi^2}}\mathrm{d}\xi=\pm\sqrt{1+K_1g^2}=K_1\chi+K_2 \qquad (102)$$

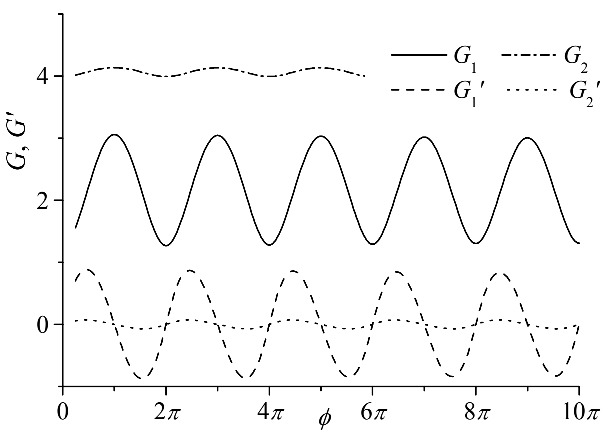

Fig. 5 Sample plot of the periodic results of the nonlinear type III solution for the specific case of $\lambda=-3$ and $C=1$. The two cases illustrate the solution multiplicity with different initial conditions.

hence $1+K_1g^2=(K_1\chi+K_2)^2$ or

$$g(\chi)=\pm\sqrt{[(K_1\chi+K_2)^2-1]/K_1} \qquad (103)$$

Finally, the type III solution gives

$$G(\phi)=\pm C^{1/4}\left[\frac{(K_1\cos\phi+K_2)^2-1}{K_1}\right]^{1/2} \qquad (104)$$

and so, in combination with Eqs. (90) and (84), renders

$$\psi(R,\phi)=\pm C^{1/4}R\left[\frac{(K_1\cos\phi+K_2)^2-1}{K_1}\right]^{1/2} \qquad (105)$$

with

$$u_R=\mp\frac{C^{\frac{1}{4}}K_1^{1/2}(K_1\cos\phi+K_2)}{R\left[(K_1\cos\phi+K_2)^2-1\right]^{\frac{1}{2}}} \qquad (106)$$

$$u_\phi=\mp\frac{C^{\frac{1}{4}}\left[(K_1\cos\phi+K_2)^2-1\right]^{1/2}}{K_1^{1/2}R\sin\phi} \qquad (107)$$

This particular profile cannot be made to observe the boundary conditions implied in the bidirectional vortex. However, it may find useful application elsewhere.

IV. Sample Verification

To verify that the bidirectional vortex is valid inside a cylinder, it can be compared to its equivalent obtained by Vyas, Majdalani and Chiaverini.[29] In order to do so, one can employ the coordinate transformations $R\cos\phi=z$ and $R\sin\phi=r$. The corresponding velocities are related vis-à-vis

$$\begin{cases}u_r=u_R\sin\phi+u_\phi\cos\phi\\ u_z=u_R\cos\phi-u_\phi\sin\phi\end{cases} \qquad (108)$$

or, in matrix form

$$\begin{bmatrix}u_r\\u_z\end{bmatrix}=\begin{bmatrix}\sin\phi & \cos\phi\\ \cos\phi & -\sin\phi\end{bmatrix}\begin{bmatrix}u_R\\u_\phi\end{bmatrix} \qquad (109)$$

One may recall from basic analysis that the inverse of this coefficient matrix is the matrix itself; for we also have

$$\begin{bmatrix}u_R\\u_\phi\end{bmatrix}=\begin{bmatrix}\sin\phi & \cos\phi\\ \cos\phi & -\sin\phi\end{bmatrix}\begin{bmatrix}u_r\\u_z\end{bmatrix} \qquad (110)$$

Transformation of the spherical solution yields

$$\begin{aligned}u_r=&\left\{(K_1/R)\left[2\pi a^{-2}R^2\cos^2\phi\cos\left(\pi a^{-2}R^2\sin^2\phi\right)\right.\right.\\&\left.\left.-\sin\left(\pi a^{-2}R^2\sin^2\phi\right)\right]\right\}\sin\phi+\left\{\tfrac{-K_1}{R}\left[2\pi a^{-2}R^2\right.\right.\\&\times\cos\phi\sin\phi\cos\left(\pi a^{-2}R^2\sin^2\phi\right)\\&\left.\left.+\cot\phi\sin\left(\pi a^{-2}R^2\sin^2\phi\right)\right]\right\}\cos\phi\end{aligned}$$

$$= \frac{-K_1}{R\sin\phi}\sin\left(\pi a^{-2}R^2\sin^2\phi\right) \tag{111}$$

which, from Eq. (78), simplifies into

$$u_r = \frac{-UA_i\sin\left(\pi a^{-2}R^2\sin^2\phi\right)}{2\pi LR\sin\phi\sin\left(\pi a^{-2}b^2\right)} = \frac{-UA_i\sin\left(\pi a^{-2}r^2\right)}{2\pi Lr\sin\left(\pi\beta^2\right)} \tag{112}$$

where $\beta = b/a$. Similarly, one finds

$$u_z = 2\pi a^{-2}K_1 z\cos\left(\pi a^{-2}r^2\right) = \frac{UA_i z\cos\left(\pi a^{-2}r^2\right)}{La^2\sin\left(\pi a^{-2}b^2\right)} \tag{113}$$

and, from Eq. (17),

$$u_\theta = \frac{UR_i\sin\phi_i}{R\sin\phi} = \frac{UR_i\sin\phi_i}{r} = \frac{Ua}{r} \tag{114}$$

To render Eqs. (112)–(114) dimensionless, one may use

$$\bar{r} = \frac{r}{a}, \bar{z} = \frac{z}{a}, \bar{u}_r = \frac{u_r}{U}, \bar{u}_\theta = \frac{u_\theta}{U}, \bar{u}_z = \frac{u_z}{U}, \frac{A_i}{a^2} = \sigma^{-1} \tag{115}$$

The resulting normalized velocities become

$$\bar{u}_r = \frac{-\sin\left(\pi\bar{r}^2\right)}{2\pi\sigma l\bar{r}\sin\left(\pi\beta^2\right)} = -\frac{\kappa}{\bar{r}}\frac{\sin\left(\pi\bar{r}^2\right)}{\sin\left(\pi\beta^2\right)} \tag{116}$$

$$\bar{u}_\theta = \frac{1}{\bar{r}} \tag{117}$$

$$\bar{u}_z = \frac{\bar{z}\cos\left(\pi\bar{r}^2\right)}{\sigma l\sin\left(\pi\beta^2\right)} = 2\pi\kappa\bar{z}\frac{\cos\left(\pi\bar{r}^2\right)}{\sin\left(\pi\beta^2\right)} \tag{118}$$

where $\kappa = (2\pi\sigma l)^{-1}$ is the tangential inlet parameter. It should be noted that, in order for the outflow radius to match that of the nozzle inlet, the radius of the latter should be $b = a/\sqrt{2}$ or $\beta = 1/\sqrt{2}$. Under these idealized conditions, the bidirectional vortex becomes expressible by

$$\bar{u}_r = -\frac{\kappa}{\bar{r}}\sin\left(\pi\bar{r}^2\right), \bar{u}_\theta = \frac{1}{\bar{r}}, \bar{u}_z = 2\pi\kappa\bar{z}\cos\left(\pi\bar{r}^2\right) \tag{119}$$

Equation (119) is identical to the non-dimensional solution obtained by Vyas, Majdalani and Chiaverini.[29] This converted result lends support to the validity of the current approach. For illustration, the velocity distribution is reproduced in Fig. 6. Here, the axial velocity profiles are plotted at four equally spaced axial stations. These confirm the location of the mantle, where the vortex switches polarity (at 0.707 of the chamber radius). The hyperbolic relation exhibited by the azimuthal velocity reflects the presence of a free vortex in a frictionless environment. Finally, the radial velocity component shown at several chamber aspect ratios confirms the inevitable mass transport between the outer and inner vortex regions. This crossflow is uniformly distributed along the chamber length.

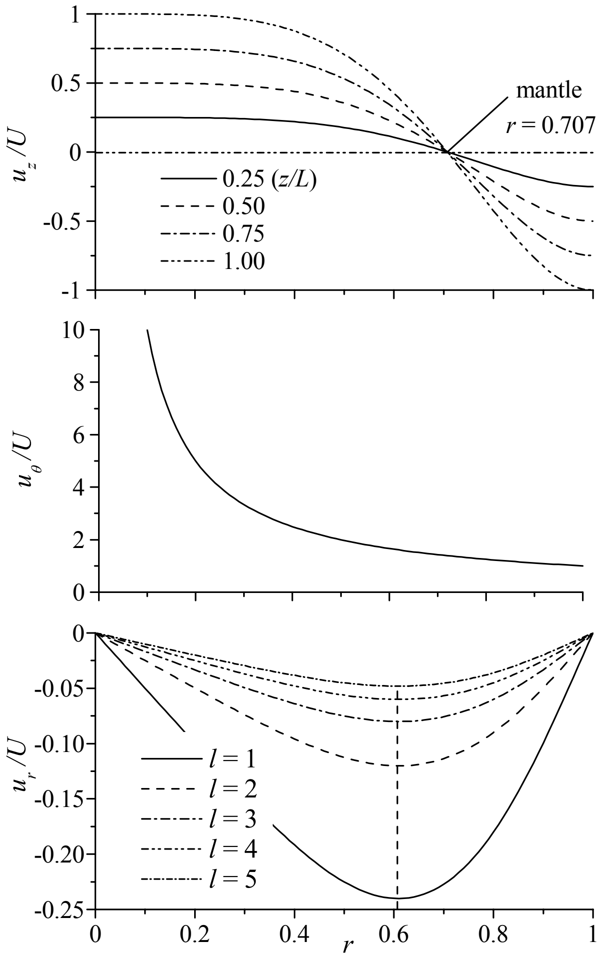

Fig. 6 Illustration of the velocity profile corresponding to the bidirectional vortex.

V. Concluding Remarks

In this paper we have uncovered several solutions in the context of steady, axisymmetric, incompressible, and inviscid vortex motion exhibiting a two-cell structure. In addition to the quest for generalizations, the focus has been on those specific solutions that will satisfy the physical conditions associated with a single pass, bidirectional vortex. In so doing, separation of variables was used in conjunction with the method of characteristics and the variation of parameters technique.

In addition to the importance of identifying the different types of possible solutions, the work's development in spherical coordinates increases our repertoire of procedural steps and available generalizations that can be applied to other geometric shapes. Specifically, the work may prove useful in tackling those problems that are more manageable in spherical geometry. The conical cyclone may be such a case whose treatment is deferred to forthcoming study.

To verify the general approach presented here, the type I solution is shown to reproduce the potential flow past a sphere, one of the rare spherical solutions found in the technical literature. After conversion to polar-cylindrical coordinates, the type II solution is shown to reproduce the bidirectional vortex in a straight cylinder. As the latter is obtained in inviscid form, it unravels the free vortex motion that is known to affect the bulk flow away from the core. Near the chamber axis, viscous stresses rise in importance as transition to a forced vortex becomes inevitable.[31] The treatment of attendant structures in spherical geometry is hoped to be accomplished in later work. The discussion of other possible solutions arising with single or multiple flow passes is also hoped to receive attention in similar geometry. Finally, in the forced vortex analysis, incorporation of viscous terms will be needed to capture the core motion. Similar work will be necessary to carefully capture the boundary layers adjacent to the endwall and sidewall. It is hoped that their analysis will open up additional lines of research inquiry.

Appendix A: Conical Geometry

By placing the origin of the spherical coordinate system at the center of the head end (i.e. the short side of the truncated cone in Fig. 7), one may define the normal and tangential velocity components (u_n, u_t) to be normal and tangential to the sidewall, respectively. Here, the sidewall is tapered at an angle α with respect to the axis. It is easy to show that

$$\begin{bmatrix} u_n \\ u_t \end{bmatrix} = \begin{bmatrix} \sin(\phi-\alpha) & \cos(\phi-\alpha) \\ \cos(\phi-\alpha) & -\sin(\phi-\alpha) \end{bmatrix} \begin{bmatrix} u_R \\ u_\phi \end{bmatrix} \qquad \text{(A1)}$$

Another geometric property of importance is the relation between the spherical radius R and the colatitude angle ϕ along the sidewall. By applying the sine law to an arbitrary triangle anchored at the sidewall, one finds

$$\frac{R}{\sin\left(\frac{1}{2}\pi+\alpha\right)} = \frac{a}{\sin(\phi-\alpha)} \text{ or } R = \frac{a\cos\alpha}{\sin(\phi-\alpha)} \qquad \text{(A2)}$$

If this coordinate system is adopted, then the no flow boundary condition becomes

$$u_n = u_R \sin(\phi-\alpha) + u_\phi \cos(\phi-\alpha) = 0 \qquad \text{(A3)}$$

This is true along the sidewall defined by $R = a\cos\alpha\csc(\phi-\alpha)$. Similar work is required to set up the remaining boundary conditions and solve the corresponding problem in a conical cyclone.

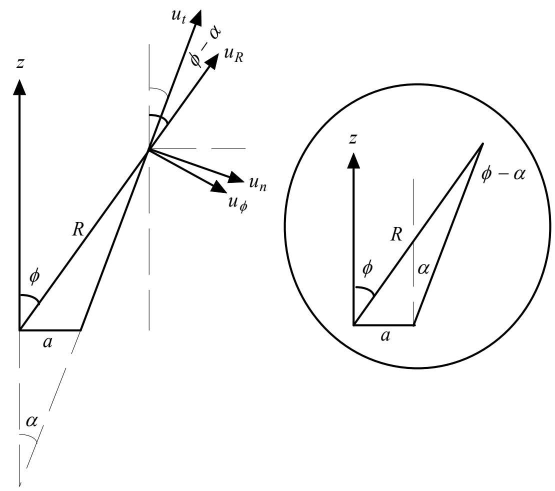

Fig. 7 Spherical coordinates applied to a conical chamber.

Acknowledgments

This project was sponsored, in part, by the Faculty Early Career Development (CAREER) Program of the National Science Foundation under Grant No. CMS-0353518. The first two authors wish to express their immense gratitude to the Program Director, Dr. Masayoshi Tomizuka, Dynamic Systems and Control. His fostering of national and international collaboration is gratefully acknowledged. The authors also wish to extend their sincere appreciation to the program participants whose indirect comments and suggestions have made this work possible.

References

[1]ter Linden, A. J., "Investigations into Cyclone Dust Collectors," *Proceedings of the Institution of Mechanical Engineers,* Vol. 160, 1949, pp. 233-251.

[2]Kelsall, D. F., "A Study of Motion of Solid Particles in a Hydraulic Cyclone," *Transactions of the Institution of Chemical Engineers,* Vol. 30, 1952, pp. 87-103.

[3]Smith, J. L., "An Experimental Study of the Vortex in the Cyclone Separator," *Journal of Basic Engineering-Transactions of the ASME*, 1962, pp. 602-608.

[4]Smith, J. L., "An Analysis of the Vortex Flow in the Cyclone Separator," *Journal of Basic Engineering-Transactions of the ASME*, 1962, pp. 609-618.

[5]Fontein, F. J., and Dijksman, C., *Recent Developments in Mineral Dressing*, Institution of Mining and Metallurgy, London, 1953, p. 229.

[6]Bloor, M. I. G., and Ingham, D. B., "Theoretical Investigation of the Flow in a Conical Hydrocyclone," *Transactions of the Institution of Chemical Engineers,* Vol. 51, 1973, pp. 36-41.

[7]Bloor, M. I. G., and Ingham, D. B., "On the Use of Pohlhausen Method in Three Dimensional Boundary Layers," *Zeitschrift für angewandte Mathematik und Physik,* Vol. 28, 1977, pp. 289-299.

[8]Bloor, M. I. G., and Ingham, D. B., "The Flow in Industrial Cyclones," *Journal of Fluid Mechanics,* Vol. 178, 1987, pp. 507-519.

[9]Reydon, R. F., and Gauvin, W. H., "Theoretical and Experimental Studies of Confined Vortex Flow," *The Canadian Journal of Chemical Engineering,* Vol. 59, 1981, pp. 14-23.

[10]Vatistas, G. H., Lin, S., and Kwok, C. K., "Theoretical and Experimental Studies on Vortex Chamber Flows," *AIAA Journal,* Vol. 24, No. 4, 1986, pp. 635-642.

[11]Vatistas, G. H., Lin, S., and Kwok, C. K., "Reverse Flow Radius in Vortex Chambers," *AIAA Journal,* Vol. 24, No. 11, 1986, pp. 1872-1873.

[12]Vatistas, G. H., "Tangential Velocity and Static Pressure Distributions in Vortex Chambers," *AIAA Journal,* Vol. 25, No. 8, 1987, pp. 1139-1140.

[13]Hsieh, K. T., and Rajamani, R. K., "Mathematical Model of the Hydrocyclone Based on Physics of Fluid Flow," *AIChE Journal,* Vol. 37, No. 5, 1991, pp. 735-746.

[14]Hoekstra, A. J., Derksen, J. J., and Van den Akker, H. E. A., "An Experimental and Numerical Study of Turbulent Swirling Flow in Gas Cyclones," *Chemical Engineering Science,* Vol. 54, 1999, pp. 2055-2065.

[15]Derksen, J. J., and Van den Akker, H. E. A., "Simulation of Vortex Core Precession in a Reverse-Flow Cyclone," *AIChE Journal,* Vol. 46, No. 7, 2000, pp. 1317-1331.

[16]Fang, D., Majdalani, J., and Chiaverini, M. J., "Simulation of the Cold-Wall Swirl Driven Combustion Chamber," AIAA Paper 2003-5055, July 2003.

[17]Smagorinsky, J., "General Circulation Experiments with the Primitive Equations: 1. The Basic Experiment," *Monthly Weather Review,* Vol. 91, 1963, p. 99.

[18]Lilley, D. G., "Swirl Flows in Combustion: A Review," *AIAA Journal,* Vol. 15, No. 8, 1977, pp. 1063-1078.

[19]Boysan, F., Ayers, W. H., and Swithenbank, J., "A Fundamental Mathematical Modelling Approach to Cyclone Design," *Institute of Chemical Engineers,* Vol. 60, 1982, p. 222.

[20]Gupta, A. K., Lilley, D. G., and Syred, N., *Swirl Flows*, Abacus, London, UK, 1984.

[21]Zhou, L. X., and Soo, S. L., "Gas-Solids Flow and Collection of Solids in a Cyclone Separator," *Power Technology,* Vol. 63, 1990, p. 45.

[22]Dyakowski, T., and Williams, R. A., "Modelling Turbulent Flow within a Small-Diameter Hydrocyclone," *Chemical Engineering Science,* Vol. 48, 1993, p. 1143.

[23]Yazdabadi, P. A., Griffiths, A. J., and Syred, N., "Characterization of the Pvc Phenomena in the Exhaust of a Cyclone Dust Seperator," *Experiments in Fluids,* Vol. 17, 1994, pp. 84-95.

[24]Elgobashi, S., "On Predicting Particle-Laden Turbulent Flows," *Applied Scientific Research,* Vol. 52, 1994, p. 309.

[25]Griffiths, A. J., Yazdabadi, P. A., and Sred, N., "Alternative Eddy Shedding Set up by the Nonaxisymmetric Recirculation Zone at the Exhaust of a Cyclone Dust Separator," *Journal of Fluids Engineering,* Vol. 120, 1998, p. 193.

[26]Chiaverini, M. J., Malecki, M. J., Sauer, J. A., and Knuth, W. H., "Vortex Combustion Chamber Development for Future Liquid Rocket Engine Applications," AIAA Paper 2002-2149, July 2002.

[27]Chiaverini, M. J., Malecki, M. J., Sauer, J. A., Knuth, W. H., and Hall, C. D., "Final Report on Cold-Wall Vortex Combustion Chamber-a Phase I SBIR Project," Orbital Technological Corporation, NASA Contact No. NAS8-01073 Rept. OTC-GS0107-01-1, August 2001.

[28]Chiaverini, M. J., Malecki, M. M., Sauer, J. A., Knuth, W. H., and Hall, C. D., "Testing and Evaluation of Vortex Combustion Chamber for Liquid Rocket Engines," JANNAF 2002.

[29]Vyas, A. B., Majdalani, J., and Chiaverini, M. J., "The Bidirectional Vortex. Part 1: An Exact Inviscid Solution," AIAA Paper 2003-5052, July 2003.

[30]White, F. M., *Viscous Fluid Flow*, McGraw-Hill, New York, 1991, pp. 135-136.

[31]Vyas, A. B., Majdalani, J., and Chiaverini, M. J., "The Bidirectional Vortex. Part 2: Viscous Core Corrections," AIAA Paper 2003-5053, July 2003.